Appl. Phys. B 56, 3–7 (1993)

Applied Physics B Photophysics and Laser Chemistry

Verification of X-Ray Line Coincidences by High-Resolution Spectroscopy

K. Gäbel [1], **Ch. Bergmann** [2], **E. Fill** [2], **E. Förster** [1], **and I. Uschmann** [1]

[1] Friedrich-Schiller-Universität Jena, O-6900 Jena, Fed. Rep. Germany
[2] Max-Planck-Institut für Quantenoptik, W-8046 Garching, Fed. Rep. Germany (Fax: +49-89/32905-200)

Received 18 September 1992/Accepted 16 October 1992

Abstract. Photo-resonant pumping of X-ray lasers requires close coincidence of a strong emission line with a suitable absorbing transition. We use a high-resolution crystal spectrometer to verify five coincidences, one of which has apparently not yet appeared in published work. All but one of the coincidences are found to lie within one linewidth. With respect to X-ray laser photo-pumping three of the five coincidences seem to be promising candidates.

PACS: 42.55.Vc, 32.30.Rj, 52.25.Nr

The renewed interest in photo-resonant pumping of X-ray lasers has two main reasons: Firstly, the wavelength scaling of this pumping method is predicted to be superior to that achieved by other excitation methods [1–4] and, secondly, good-enough line coincidences may be more abundant than is generally believed [5–8]. The recently reported indications for photo-resonantly pumped lasers [9, 10] support this assertion.

Photo-resonant pumping requires that a strong emission line of an ion be coincident with an absorbing transition with a suitable upper laser level. In the following, these transitions will be called the pumping and the collecting transitions, respectively. Considerable efforts have been made to find suitable line coincidences and quite a number of compilations exist (see, for example, [11–15]). Only part of the listed line pairs, however, meet the following stringent requirements:

1. The pumping line must be a strong, prominent line, possibly a resonance line of a hydrogenic or helium-like ion.

2. Since typical relative Doppler widths in a laser plasma are $\Delta\lambda/\lambda = 3 \times 10^{-4}$, coincidence in approximately the same range is required in order to get sufficient overlap of the two lines.

Condition 2 is the more restrictive one. It may be somewhat relaxed by taking advantage of the following effects:

- opacity broadening of the pumping line,
- dynamic Doppler shift in moving plasmas,
- Stark broadening by the ionic plasma field or the laser field.

Simple estimates suggest that a suitably designed experiment may result in a tolerable wavelength mismatch of two to three Doppler widths, thus considerably increasing the number of useful coincidences.

1 Motivation for Line-Coincidence Verification

An inevitable feature of coincidence compilations is that the wavelengths of the lines are taken from the works of different authors. It is often the case that one line is derived from experimental and the other from theoretical investigations. Since absolute wavelengths are only known with an accuracy of typically 10^{-3} at best, the error in the wavelength mismatch renders many of the listed coincidences useless. (For notable exceptions see [8, 12].) It is important to realize that only a measurement of the *relative* wavelengths is required, but with a resolution and accuracy comparable to the linewidth.

In this work we report the results of an experimental effort to verify five coincidences (see Table 1). The choice of the coincidences was governed by the condition that the wavelengths be in the region of the quartz-crystal spectrometer ($\lambda < 2d = 8.51$ Å), satisfy criterion 1 and have a good chance of satisfying criterion 2.

Note that the relative wavelength mismatch listed in the Table is defined as $(\lambda_p - \lambda_c)/\lambda_p$, where λ_p and λ_c are the wavelengths of the pump and collecting line, respectively. With this definition the relative wavelength mismatch may be positive or negative and the sign indicates how the line overlap can be improved by the dynamic Doppler shift: a negative relative wavelength mismatch means that the resonance is improved if the pumping and absorbing plasmas stream away from each other, whereas a positive wavelength mismatch requires counter-streaming plasmas.

2 Experimental Arrangement

High-power laser radiation was focused onto solid targets and the X-ray spectra of the emission were recorded. Two different lasers were employed:

Table 1. Coincidences investigated. λ_p, λ_c, λ_l: Wavelengths of pumping, collecting and lasing lines. $\Delta\lambda_p$, $\Delta\lambda_c$: Experimental linewidths (FWHM) of pumping and collecting lines. $(\lambda_p - \lambda_c)/\lambda_p$: Experimental relative wavelength mismatch and (in brackets) relative wavelength mismatch from [14, 15, 21–24]. I_p: Intensity of pumping line emitted at the target into 2π

Pumping transition	Collecting transition	λ_p [Å]	λ_l [Å]	$\Delta\lambda_p/\lambda_p$ [10^{-4}]	$\Delta\lambda_c/\lambda_c$ [10^{-4}]	$(\lambda_p - \lambda_c)/\lambda_p$ [10^{-4}]	I_p [10^{11} W/cm^2]
Si XIII 2^1P–1^1S He_α	Al XII 1^1S–3^1P He_β	6.65	44	8.4 ± 1.7	8.0 ± 1.6	$+23 \pm 3$ (+19)	0.49[a]
Si XIV $2P_{3/2}$–1 L_α	Al XII 1^1S–5^1P He_δ	6.18	275 87.5	7.9 ± 1.3	10.0 ± 2	$+10 \pm 2$ (+8)	0.25[a]
S XV 3^1P–1^1S He_β	P XV 1–4 L_γ	4.3	83.2	13.7 ± 2.7	19.1 ± 4	-15 ± 2 (−21)	1.0[b]
K XVIII 2^1P–1^1S He_α	Cl XVII 1–3 L_β	3.53	22.5	11.9 ± 2.4	11.6 ± 2.4	-3 ± 1 (−4.6)	1.3[b]
K XIX $2P_{1/2}$–1 L_α	Cl XVII 1–4 L_γ	3.35	64.7 16.8	12 ± 2.4		– (+3)	0.17[b]

[a] Irradiation intensity 10^{14} W/cm^2, $\lambda = 1.315\,\mu$m [b] Irradiation intensity 5×10^{15} W/cm^2, $\lambda = 1.315\,\mu$m

a) A Nd-glass laser with a pulse energy of 10 J in 3 ns at the second harmonic ($\lambda = 530$ nm). The pulse, focused to a spot 50 µm in diameter resulted in a power density on the target of 1.5×10^{14} W/cm^2.

b) The ASTERIX IV high-power iodine laser emitting 100 J in 450 ps at a wavelength of 1.315 µm [16]. By irradiation in the best focus position (70 µm spot diameter) an intensity of 6×10^{15} W/cm^2 could be reached on the target.

A Johann crystal spectrometer was used in our experiments to reduce the influence of the source size and thus improve the spectral resolution [17]. The spectrometer viewed the target at an angle of 45° from a distance of approximately 10 cm. Two quartz crystals with different crystallographic orientation, resulting in different lattice spacings ($2d = 6.6864$ Å and $2d = 8.5096$ Å) were used. They were specially selected by X-ray topographic methods in order to eliminate material with structural defects. The crystals were bent to a radius of 144 mm.

The influence of the source size on resolution was determined theoretically by means of a ray-tracing code and experimentally using the point focus of an X-ray tube emitting the Cu–K_α line. It was found that up to a source size of approximately 75 µm the resolution of the spectrometer was only limited by the width of the rocking curve [18].

The spectral resolution is then obtained by transforming the FWHM angle $\Delta\Theta_{RC}$ of the rocking curve to the wavelength scale according to the differential Bragg equation

$$\lambda/\Delta\lambda = \tan(\Theta_B)/\Delta\Theta_{RC}\,, \tag{1}$$

where Θ_B is the Bragg angle. Under the conditions of our experiment a spectral resolution of 5000 is calculated.

Absolutely calibrated ORWO X-ray film was used for recording. Various aluminum and carbon filters were placed in front of the film in order to get a suitable optical density.

To verify coincidence between a pump line of material A and a collecting line of material B, the following procedure was applied:

- Spectra of A and B were recorded on separate film.
- Spectra of A and B were recorded on the same film.
- A spectrum of a compound target containing both A and B was recorded.

The evaluation of the spectra was performed by means of a digital densitometer taking into account a minimum of 3 shots for each of the above mentioned conditions. Gaussian or Lorentzian lineshape functions were fitted to the data and the results were derived from the better fit. Absolute emission intensities of the pump lines into 2π were calculated with the equation

$$I_p = \kappa E_f (A_f/A_t)(\tau T_f R_{int} \Phi/\pi)^{-1}\,, \tag{2}$$

where I_p = intensity emitted at target surface into 2π, κ = correction factor of order unity which takes the focusing properties of the bent crystal into account, E_f = energy density on the film, A_f = area of the recorded line on the film, A_t = area of the emitting spot on the target, τ = duration of the emission, taken to be equal to the duration of the exciting laser pulse (450 ps), T_f = filter transmission, R_{int} = integrated crystal reflectivity, Φ = planar angle of the line on the film as seen from the target.

3 Results

The main experimental results for the five coincidences, i.e., the relative linewidths $\Delta\lambda/\lambda$, the relative line mismatches $(\lambda_p - \lambda_c)/\lambda_p$ and the intensities of the pumping lines are listed in Table 1. To simplify the notation, resonance lines of helium-like ions will be referred to as He_α, He_β, etc., meaning the transitons $2^1P \leftrightarrow 1^1S$, $3^1P \leftrightarrow 1^1S$ and so on. For the resonance lines of hydrogenic ions L_α, L_β, etc. will be written. If necessary, the j-value of the upper level will be indicated.

It is evident by comparing the two values for $(\lambda_p - \lambda_c)/\lambda_p$ given in Table 1, that there is good agreement between the

wavelength mismatches measured in this work and their values taken from the literature. This reflects the high standard of accuracy of wavelength measurements in this region.

It was observed that the generation of helium-like lines required considerably lower laser intensities than that of hydrogenic lines. This is in accord with the observations of Aglitskii et al. [19] and Phillion and Hailey [20]. In [19] no hydrogenic lines beyond sulphur are reported. In [20] L_α of chlorine is recorded at an irradiation intensity of 1.5×10^{15} W/cm^2.

All of the lines were observed to be broadened considerably beyond the Doppler width. Since the recorded spectra were time-integrated, part of the broadening may be due to a bulk Doppler shift. A detailed discussion of the features of the various resonances will be given in the following.

3.1 The Silicon–Aluminum Resonances (Si–He$_\alpha$ → Al–He$_\beta$ *and* Si–L$_\alpha$ → Al–He$_\delta$)

For the investigation of these spectra relatively moderate intensities were needed since both the He-like and H-like lines of Al and Si can be observed at intensities on target below 10^{14} W/cm^2. Figure 1 shows separate spectra of Al and Si and the spectrum of a compound target consisting of a 1000 Å layer of Al on Si.

It is evident that the Si–He$_\alpha$ pump line does not coincide with the Al–He$_\beta$ collecting line, indicating – as expected – that the wavelength mismatch is larger than the linewidths.

The conclusions from the single-shot spectra are confirmed by recording on the same film one shot on silicon and 3 shots on aluminum (in order to enhance the aluminum spectrum). The Si–He$_\alpha$ and Al–He$_\beta$ lines are well resolved, indicating that the line mismatch is considerably larger than the linewidths.

A numerical evaluation of the experimental data for the two lines is shown in Fig. 2, and demonstrates the insufficient overlap. We note that a Lorentzian line shape gives a better fit to the data than a Gaussian one, consistently with the observation that the lines are broadened beyond the Doppler width.

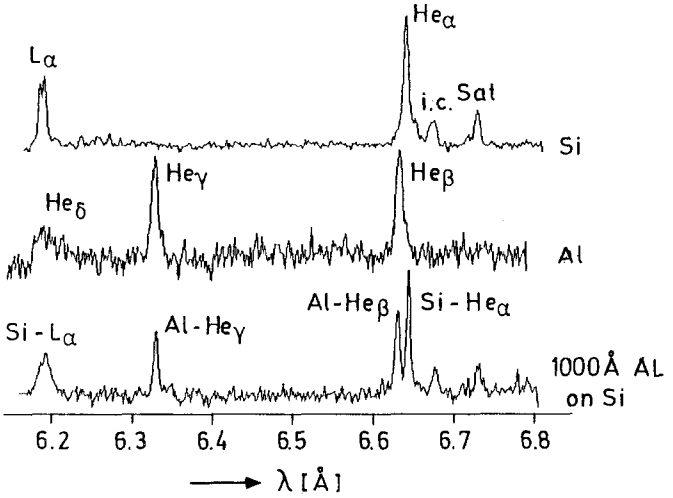

Fig. 1. X-ray spectra relevant to the Si → Al coincidences. *Top:* spectrum of Si; *middle:* spectrum of Al; *bottom:* spectrum of a target consisting of 1000 Å Al on Si (sat.: satellite; i.c.: intercombination line)

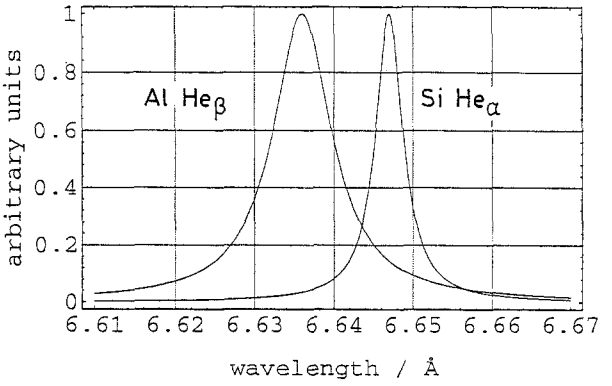

Fig. 2. Numerical fit to experimental spectra: overlap of the Si–He$_\alpha$–Al–He$_\beta$ lines. Lorentzians are used for fitting

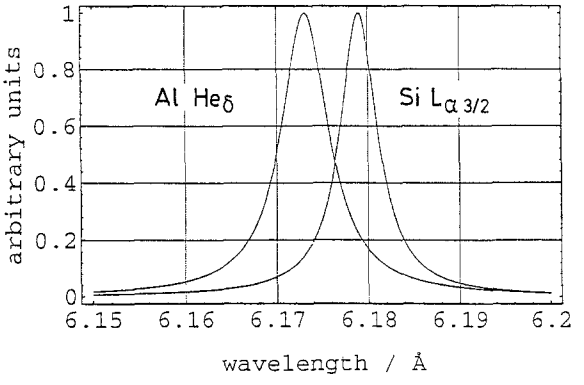

Fig. 3. Numerical fit (Lorentzians) to experimental spectra: overlap of the Si–L$_{\alpha_{3/2}}$–Al–He$_\delta$ lines

The Si–L$_\alpha$ → Al–He$_\delta$ coincidence is better than the previous one. To our knowledge, it is reported here for the first time. In Fig. 3 a numerical fit to the experimental spectra shows the overlap of the two lines. Again, Lorentzians give a better fit to the experimental data.

3.2 The Sulphur–Phosphorus Resonance (S–He$_\beta$ → P–L$_\gamma$)

The lines of He-like sulphur could readily be generated at the relatively low intensities provided by the Nd-glass laser. To see the L$_\gamma$ line of phosphorus, however, the iodine laser had to be used. The reason, as mentioned above, is that the generation of H-like lines requires considerably higher intensities than that of He-like ones. It is important to realize that seeing the collecting line in emission is only necessary to *verify* a coincidence. For photo-resonant pumping only the ground state of the collecting line must be generated.

The spectra of pure sulphur, of pure phosphorus and of P_4S_3 are shown in Fig. 4. Evaluation of the spectra of the pure substances and comparison with the spectrum of the compound show that the resonance S–He$_\beta$ → P–L$_\gamma$ may indeed be a useful one. The spectral overlap of the two lines is demonstrated in Fig. 5. Numerical values of the linewidths and the wavelength mismatch are given in Table 1. Note that for this coincidence the overlap may be improved by

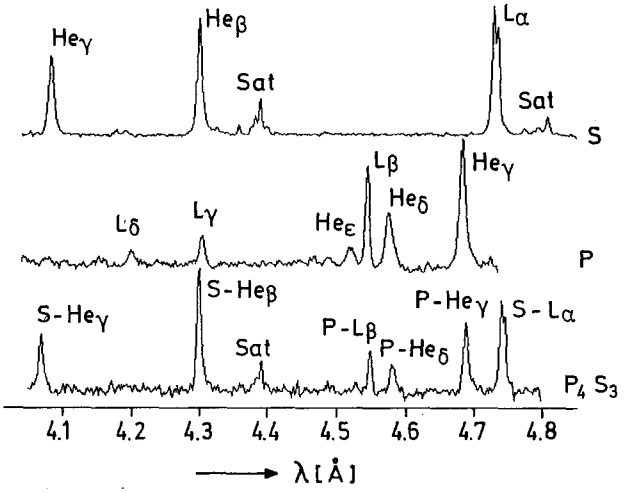

Fig. 4. Spectra relevant to the S → P coincidence. *Top:* spectrum of S; *middle:* spectrum of P; *bottom:* spectrum of P_4S_3

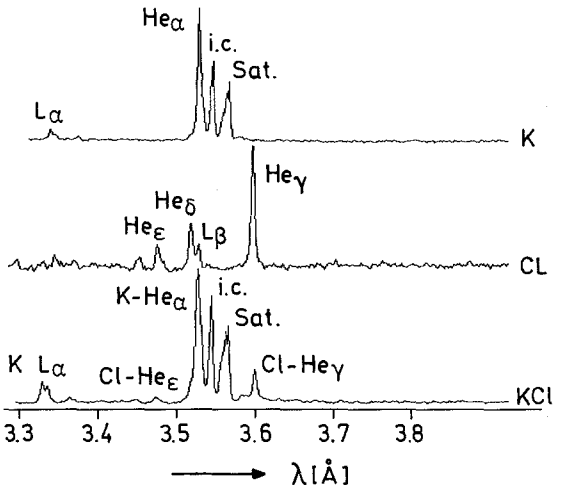

Fig. 6. Spectra relevant to the K → Cl coincidences. *Top:* spectrum of K; *middle:* spectrum of Cl; *bottom:* spectrum of KCl

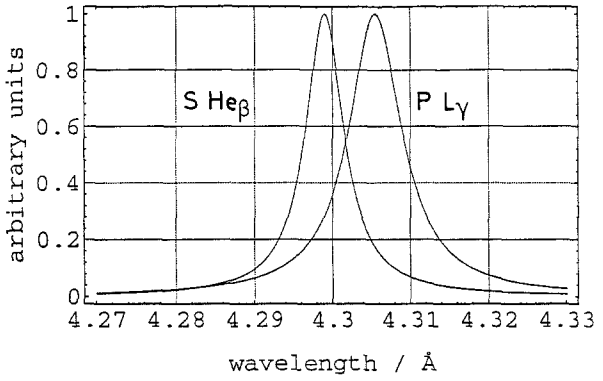

Fig. 5. Numerical fit (Lorentzians) to experimental spectra: overlap of the S–He_β and P–L_γ lines

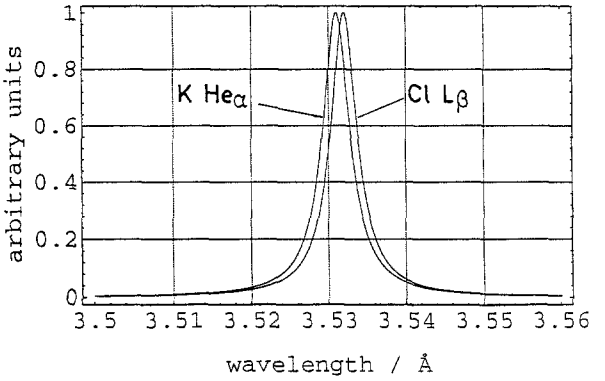

Fig. 7. Numerical fit (Lorentzians) to experimental spectra: overlap of the K–He_α and Cl–L_β lines

the dynamic Doppler shift in plasmas streaming apart from each other.

3.3 The K–Cl *Resonances* (K–$He_\alpha \rightarrow$ Cl–L_β *and* K–$L_\alpha \rightarrow$ Cl–L_γ)

Intense emission of He-like lines of both Cl and K was already observed at target irradiation below 10^{14} W/cm^2. Again, intensities above 10^{15} W/cm^2 were required for the observation of hydrogenic lines.

A spectrum of K alone was obtained with a KDP crystal as a target. (The phosphorus lines do not overlap with the resonance lines of K.) This spectrum is shown in Fig. 6. The structure of the He_α line is typical of these lines at comparable nuclear charge. Its various components, including satellites, intercombination and forbidden lines, can be identified with the aid of [19]. The strongest emission is due to the 2^1P–1^1S resonance line, but the intercombination line and some of the satellites are emitted at comparable intensities.

The K–L_α line is rather weak compared with the He-like lines. Again, its fine structure is resolved and the line originating from the $j = 1/2$ level is broader than that from $j = 3/2$.

To obtain a spectrum of Cl, an NaCl crystal was used as target (Fig. 6). The emission of Na does not interfere with the Cl resonance lines. The feature at the short-wavelength side of the He_γ line consists of a hydrogenic and a He-like line, L_β and He_δ. The first one is the collecting line for the K–He_β pump line.

A compound spectrum was generated with a KCl crystal as target (Fig. 6). The Cl–L_β line is buried in the K–He_α line, indicating an overlap within less than a linewidth. The result of a numerical evaluation of the data is shown in Fig. 7. For detailed values of linewidths and line mismatch see Table 1.

Cl–L_γ, the collecting line for the K–L_α pump line, was not observed in our spectra. However, since the position of hydrogenic lines is known quite accurately from theory [21, 22], the wavelength mismatch of this coincidence is very likely to be as given in Table 1.

4 Summary and Conclusions

The intensities given in Table 1 indicate that conversion efficiencies from laser light into a single X-ray line up to 5×10^{-4} have been observed. This is consistent with the data reported in [20] for somewhat shorter pump pulses.

The implications of these observations for photo-resonantly pumped X-ray lasers may be summarized as follows:

Si–$He_\alpha \rightarrow$ Al–He_β: The pump line is strong. Unfortunately, however, the line overlap is poor, resulting in insufficient coupling of pump photons into the collecting line. Improving the wavelength match by making use of the dynamic Doppler shift may be possible, but counter-streaming plasmas are required for this purpose.

Si–$L_\alpha \rightarrow$ Al–He_δ: The pump line is strong. Line separation is about one linewidth. This coincidence seems promising for photo-resonant pumping. However, the $\Delta n = 1$ transitions have rather long wavelengths ($\cong 275$ Å).

S–$He_\beta \rightarrow$ P–L_γ: The pump line is of medium strength. The overlap is adequate. Moderate technological effort is needed to generate targets.

K–$He_\alpha \rightarrow$ Cl–L_β: Of the resonances investigated this one is the best. The pump line is strong and the line overlap is excellent. Targets can be fabricated at ease. The wavelength of the laser transition is below the oxygen K-edge (low-wavelength end of the water window).

K–$L_\alpha \rightarrow$ Cl–L_γ: To generate the pump line with adequate strength requires laser intensities above 10^{16} W/cm^2. Thus, this line coincidence may not be useful for a practical photo-resonant pumping scheme, despite its small wavelength mismatch.

Acknowledgements. We thank G. Pfaff, Department of Chemistry, University of Jena for producing the P_4S_3 crystals. This work was supported, in part by the Commission of the European Communities in the framework of the Euratom-IPP Association.

References

1. A.V. Vinogradov, I.I. Sobelman, E.A. Yukov: Sov. J. Quantum Electron. **5**, 59 (1975)
2. B.A. Norton, N.J. Peacock: J. Phys. B **8**, 989 (1975)
3. A.V. Vinogradov, B.N. Chichkov, E.A. Yukov: Sov. J. Quantum Electron. **14**, 444 (1984)
4. B.N. Chichkov, E.E. Fill: Phys. Rev. A **42**, 599 (1990)
5. J. Nilsen: Phys. Rev. A **40**, 5440 (1989)
6. J. Nilsen: Opt. Commun. **78**, 51 (1990)
7. B.N. Chichkov, E.E. Fill: Opt. Commun. **74**, 202 (1989)
8. P. Beiersdorfer, J. Nilsen, A. Osterheld, D. Vogel, K. Wong, R.E. Marrs, R. Zasadzinski: Phys. Rev. A **46**, R 25 (1992)
9. T. Boehly, M. Russotto, R.S. Craxton, R. Epstein, B. Yaakobi, L.B. Da Silva, J. Nilsen, E.A. Chandler, D.J. Fields, B.J. MacGowan, D.L. Matthews, J.H. Scofield, G. Shimkaveg: Phys. Rev. A **42**, 6962 (1990)
10. E.E. Fill, E. Förster, K. Gäbel: Proc. Lasers '91, pp. 52–57
11. P.L. Hagelstein: Plasma Phys. **25**, 1345 (1983)
12. P.G. Burkhalter, D.A. Newman, C.J. Hailey, P.D. Rockett, G. Charatis, B.J. MacGowan, D.L. Matthews: J. Opt. Soc. Am. B **2**, 1894 (1985)
13. R.C. Elton, T.W. Lee, W.A. Molander: Phys. Rev. A **33**, 2817 (1986)
14. R.C. Elton: *X-ray lasers* (Academic, New York 1988)
15. J. Nilsen, J. Scofield, E.A. Chandler: Appl. Opt. **31**, 4950 (1992)
16. H. Baumhacker, G. Brederlow, E. Fill, H. Krause, Ch. Schrödter, S. Staehler, R. Volk, K. Witte: Proc. Conf. Lasers and Electro-Optics, Techn. Digest **11**, Baltimore (1989)
17. S. Morita: Jpn. J. Appl. Phys. **22**, 1030 (1982)
18. E. Förster, K. Gäbel, I. Uschmann: Laser Part. Beams **9**, 135 (1991)
19. E.V. Aglitskii, V.A. Boiko, S.M. Zhakharov, S.A. Pikuz, A.Ya. Faenov: Sov. J. Quantum Electron. **4**, 500 (1974)
20. D.W. Phillion, C.J. Hailey: Phys. Rev. A **34**, 4886 (1986)
21. J.D. Garcia, J.E. Mack: J. Opt. Soc. Am. **55**, 654 (1965)
22. G.W. Erickson: J. Phys. Chem. Ref. Data **6**, 831 (1977)
23. W.C. Martin, R. Zalubas: J. Phys. Chem. Ref. Data **8**, 817 (1979)
24. C. Corliss, J. Sugar: J. Phys. Chem. Ref. Data **8**, 1109 (1979)